Nanoparticle-Based Bio-Bar Codes for the Ultrasensitive Detection of Proteins

Jwa-Min Nam, *et al.*

Science **301**, 1884 (2003);
DOI: 10.1126/science.1088755

number corresponds to a bulk resistivity of 2.4×10^{-6} ohm·m for the silver nanowire. This nanowire is easily reproducible and has markedly higher conductivity than previously reported double-helix DNA–templated silver nanowires (*20*).

The 4 × 4 DNA tile can be easily programmed by varying the sticky ends to form more sophisticated arrays for applications in construction of logical molecular devices; for instance, quantum-dot cellular automata arrays may be constructed by specifically incorporating metal nanoparticles into the nanogrids. The cavities can also be used as pixels in a uniform pixel array, which could be applied to AFM visual readout of self-assembly DNA computations such as a binary counting lattice (*30*).

References and Notes

1. N. C. Seeman, *Nature* **421**, 427 (2003).
2. T. H. LaBean, in *Computational Biology and Genome Informatics*, J. T. L. Wang, C. H. Wu, P. P. Wang, Eds. (World Scientific, River Edge, NJ, 2003), p. 35.
3. E. Winfree, F. Liu, L. A. Wenzler, N. C. Seeman, *Nature* **394**, 539 (1998).
4. T. H. LaBean *et al.*, *J. Am. Chem. Soc.* **122**, 1848 (2000).
5. C. Mao, W. Sun, N. C. Seeman, *J. Am. Chem. Soc.* **121**, 5437 (1999).
6. R. Sha, F. Liu, N. C. Seeman, *Chem. Biol.* **7**, 743 (2000).
7. H. Yan, T. H. LaBean, L. Feng, J. H. Reif, *Proc. Natl. Acad. Sci. U.S.A.* **100**, 8103 (2003).
8. C. Mao, W. Sun, Z. Shen, N. C. Seeman, *Nature* **397**, 144 (1999).
9. B. Yurke *et al.*, *Nature* **406**, 605 (2000).
10. H. Yan, X. Zhang, Z. Shen, N. C. Seeman, *Nature* **415**, 62 (2002).
11. J. J. Li, W. Tan, *Nano Lett.* **2,** 315 (2002).
12. L. Feng, S. H. Park, J. H. Reif, H. Yan, *Angew. Chem. Int. Ed.*, in press.
13. L. M. Adleman, *Science* **266**, 1021 (1994).
14. Q. Liu *et al.*, *Nature* **403**, 175 (2000).
15. C. Mao, T. H. LaBean, J. H. Reif, N. C. Seeman, *Nature* **407**, 493 (2000).
16. Y. Benenson *et al.*, *Nature* **414**, 430 (2001).
17. B. S. Ravinderjit *et al.*, *Science* **296**, 499 (2002).
18. C. A. Mirkin, *Inorg. Chem* **39**, 2258 (2000).
19. A. P. Alivisatos *et al.*, *Nature* **382**, 609 (1996).
20. E. Braun, Y. Eichen, U. Sivan, G. Ben-Yoseph, *Nature* **391**, 775 (1998).
21. K. Keren *et al.*, *Science* **297**, 72 (2002).
22. F. Patolsky, Y. Weizmann, O. Lioubashevski, I. Willner, *Angew. Chem. Int. Ed.* **41**, 2323 (2002).
23. C. F. Monson, A. T. Woolley, *Nano Lett.* **3**, 359 (2003).
24. W. E. Ford, O. Harnack, A. Yasuda, J. M. Wessels, *Adv. Mater.* **13**, 1793 (2001).
25. J. Richter *et al.*, *Adv. Mater.* **12**, 507 (2000).
26. C. M. Niemeyer, W. Burger, J. Peplies, *Angew. Chem. Int. Ed.* **37**, 2265 (1998).
27. S. Xiao *et al.*, *J. Nanopart. Res.* **4**, 313 (2002).
28. N. C. Seeman, *Trends Biotechnol.* **17**, 437 (1999).
29. Materials and methods are available as supporting material on *Science* Online.
30. E. Winfree, *J. Biomol. Struct. Dyn.* **11**, 263 (2000).

31. We thank E. Winfree, P. Rothemund, and N. Papadakis for helpful advice with AFM under aqueous buffer; D. Liu for development of the metallization procedure and L. Feng for technical assistance in the thermal profile experiment; and J. Liu for providing access to his AFM instrument. This work was supported by grants from the National Science Foundation (H.Y., J.H.R., and T.H.L.) and Defense Advanced Research Projects Agency (J.H.R.) and by an industrial partners arrangement with Taiko Denki Co., Ltd. (J.H.R. and T.H.L.).

Supporting Online Material

www.sciencemag.org/cgi/content/full/301/5641/1882/DC1
Materials and Methods
Figs. S1 to S6
References

18 July 2003; accepted 21 August 2003

Nanoparticle-Based Bio–Bar Codes for the Ultrasensitive Detection of Proteins

Jwa-Min Nam,* C. Shad Thaxton,* Chad A. Mirkin†

An ultrasensitive method for detecting protein analytes has been developed. The system relies on magnetic microparticle probes with antibodies that specifically bind a target of interest [prostate-specific antigen (PSA) in this case] and nanoparticle probes that are encoded with DNA that is unique to the protein target of interest and antibodies that can sandwich the target captured by the microparticle probes. Magnetic separation of the complexed probes and target followed by dehybridization of the oligonucleotides on the nanoparticle probe surface allows the determination of the presence of the target protein by identifying the oligonucleotide sequence released from the nanoparticle probe. Because the nanoparticle probe carries with it a large number of oligonucleotides per protein binding event, there is substantial amplification and PSA can be detected at 30 attomolar concentration. Alternatively, a polymerase chain reaction on the oligonucleotide bar codes can boost the sensitivity to 3 attomolar. Comparable clinically accepted conventional assays for detecting the same target have sensitivity limits of ~3 picomdar, six orders of magnitude less sensitive than what is observed with this method.

The polymerase chain reaction (PCR) and other forms of target amplification have enabled rapid advances in the development of powerful tools for detecting and quantifying DNA targets of interest for research, forensic, and clinical applications (*1*–*3*). The development of comparable target amplification methods for proteins could substantially improve medical diagnostics and the developing field of proteomics (*4*–*7*). Although one cannot yet chemically duplicate protein targets, it is possible to tag such targets with oligonucleotide markers that can be subsequently amplified with PCR and then use DNA detection to identify the target of interest (*8*–*13*). This approach, often referred to as immuno-PCR, allows the detection of proteins with DNA markers in a variety of different formats. Thus far, all immuno-PCR approaches involve initial immobilization of a target analyte to a surface and subsequent detection with an antibody (Ab) with a DNA marker. The DNA marker is typically strongly bound to the Ab (either through covalent interactions or streptavidin-biotin binding). Although these approaches are considerable advances in protein detection, they have several drawbacks: (i) a low ratio of DNA identification sequence to detection Ab, which limits sensitivity, (ii) slow target-binding kinetics because of the heterogeneous nature of the target-capture procedure, which increases assay time and decreases assay sensitivity, (iii) complex conjugation chemistries that are required to link the Ab and DNA markers, and (iv) PCR requirements (*14*).

Herein, we report a nanoparticle-based bio–bar-code approach to detect a protein target, free prostate-specific antigen (PSA), at low attomolar concentrations (Fig. 1). PSA was chosen as the initial target for these studies because of its importance in the detection of prostate and breast cancer, the most common cancers and the second leading cause of cancer death among American men and women, respectively (*15*–*18*). Identification of disease relapse after the surgical treatment of prostate cancer using PSA as a marker present at low levels (10s of copies) could be extremely beneficial and enable the delivery of curative adjuvant therapies (*17*, *19*). Furthermore, PSA is found in the sera of breast cancer patients, and it is beginning to be explored as a breast cancer screening target (*16*). Because the concentration of free PSA is much lower in women's serum as compared to that of men, an ultrasensitive test is needed for breast cancer screening and diagnosis.

The bio–bar-code assay reported herein uses two types of probes, magnetic microparticles (MMPs, 1-μm diameter polyamine particles with magnetic iron oxide cores) functionalized with PSA monoclonal antibodies (mAbs) (Fig. 1A) (*20*) and gold nanoparticles (NP) heavily functionalized with hybridized oligonucleotides (the bio–bar codes; 5′ AC-ACAACTGTGTTCACTAGCGTTGAACGT-GGATGAAGTTG 3′) (*7*, *21*, *22*) and polyclonal detection Abs to recognize PSA (Fig. 1A) (*20*). In a typical PSA detection experiment (Fig. 1B), the gold NPs and the MMPs sandwich the PSA target, generating a com-

Department of Chemistry and Institute for Nanotechnology, Northwestern University, 2145 Sheridan Road, Evanston, IL 60201, USA

*These authors contributed equally to the work.
†To whom correspondence should be addressed. E-mail: camirkin@chem.northwestern.edu

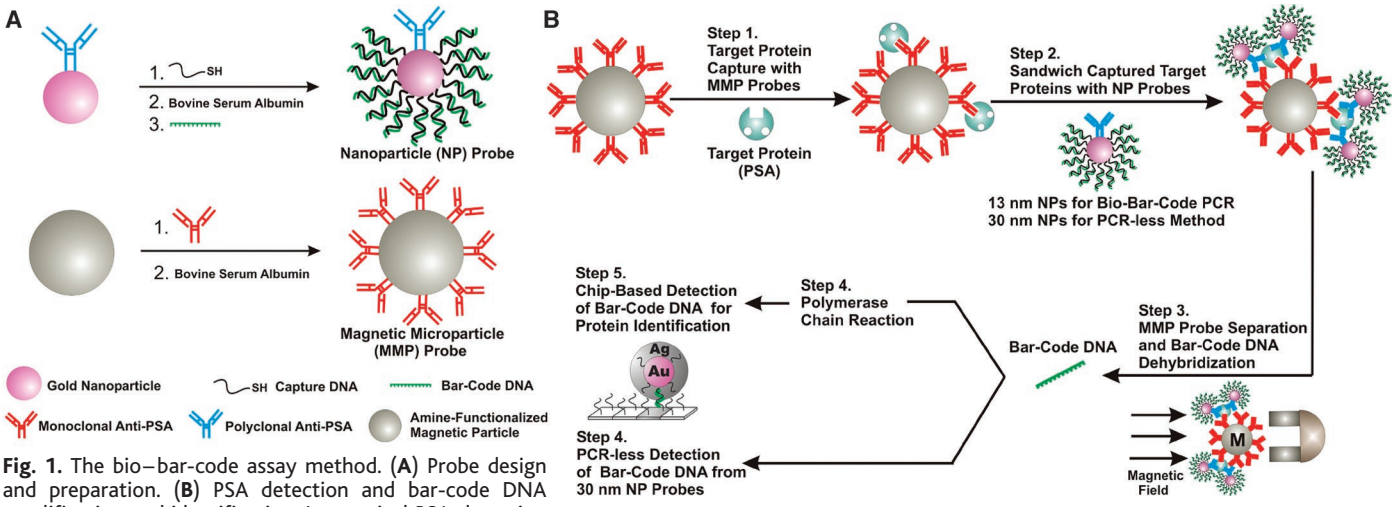

Fig. 1. The bio–bar-code assay method. (**A**) Probe design and preparation. (**B**) PSA detection and bar-code DNA amplification and identification. In a typical PSA-detection experiment, an aqueous dispersion of MMP probes functionalized with mAbs to PSA (50 μl of 3 mg/ml magnetic probe solution) was mixed with an aqueous solution of free PSA (10 μl of PSA) and stirred at 37°C for 30 min (Step 1). A 1.5-ml tube containing the assay solution was placed in a BioMag microcentrifuge tube separator (Polysciences, Incorporated, Warrington, PA) at room temperature. After 15 s, the MMP-PSA hybrids were concentrated on the wall of the tube. The supernatant (solution of unbound PSA molecules) was removed, and the MMPs were resuspended in 50 μl of 0.1 M phosphate-buffered saline (PBS) (repeated twice). The NP probes (for 13-nm NP probes, 50 μl at 1 nM; for 30-nm NP probes, 50 μl at 200 pM), functionalized with polyclonal Abs to PSA and hybridized bar-code DNA strands, were then added to the assay solution. The NPs reacted with the PSA immobilized on the MMPs and provided DNA strands for signal amplification and protein identification (Step 2). This solution was vigorously stirred at 37°C for 30 min. The MMPs were then washed with 0.1 M PBS with the magnetic separator to isolate the magnetic particles. This step was repeated four times, each time for 1 min, to remove everything but the MMPs (along with the PSA-bound NP probes). After the final wash step, the MMP probes were resuspended in NANOpure water (50 μl) for 2 min to dehybridize bar-code DNA strands from the nanoparticle probe surface. Dehybridized bar-code DNA was then easily separated and collected from the probes with the use of the magnetic separator (Step 3). For bar-code DNA amplification (Step 4), isolated bar-code DNA was added to a PCR reaction mixture (20-μl final volume) containing the appropriate primers, and the solution was then thermally cycled (*20*). The bar-code DNA amplicon was stained with ethidium bromide and mixed with gel-loading dye (*20*). Gel electrophoresis or scanometric DNA detection (*24*) was then performed to determine whether amplification had taken place. Primer amplification was ruled out with appropriate control experiments (*20*). Notice that the number of bound NP probes for each PSA is unknown and will depend upon target protein concentration.

plex with a large ratio of bar-code DNA to protein target (*23*). Application of a magnetic field draws the MMPs to the wall of the reaction vessel in a matter of seconds, allowing the separation of all of the MMPs but only the reacted NPs from the reaction mixture. Washing the aggregate structures in NANOpure water (18 megohm; Barnstead International, Dubuque, IA) dehybridizes bar-code DNA from NP-immobilized complements. With the use of the magnetic separator, we readily removed the aggregate from the assay solution to leave only the bar-code DNA, which can be quickly identified by standard DNA detection methodologies [e.g., gel electrophoresis, fluorophore-labeling, and scanometric (*24*) approaches] that may or may not rely on PCR (Fig. 1B).

Although gel electrophoresis was routinely used to analyze the results of the assay (*20*), in general the scanometric method provided higher sensitivity and was easier to implement than the gel-based method. Therefore, the results of the scanometric assay are reported herein. In the case of PCR-less detection, 30-nm gold particles were used during the detection step instead of 13-nm gold particles to increase the amount of detectable bar-code DNA (Fig. 1B, step 2). For bar-code DNA identification, chip-immobilized DNA

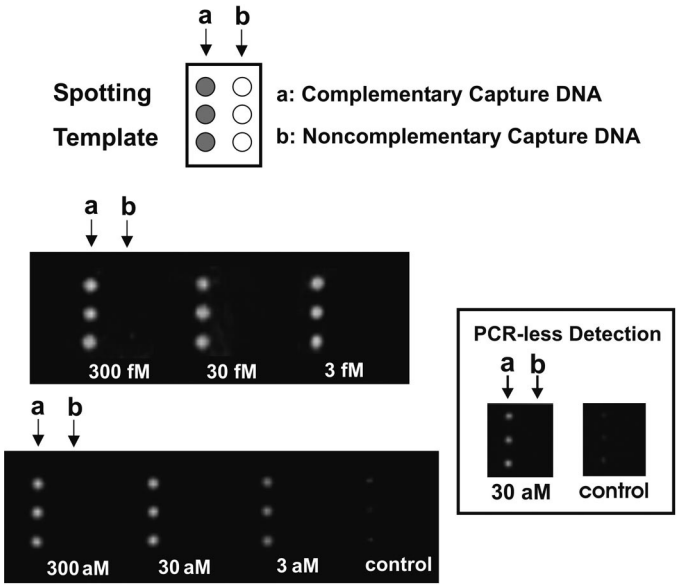

Fig. 2. Scanometric detection of PSA-specific bar-code DNA. PSA concentration (sample volume of 10 μl) was varied from 300 fM to 3 aM and a negative control sample where no PSA was added (control) is shown. For all seven samples, 2 μl of antidinitrophenyl (10 pM) and 2 μl of β-galactosidase (10 pM) were added as background proteins. Also shown is PCR-less detection of PSA (30 aM and control) with 30 nm NP probes (inset). Chips were imaged with the Verigene ID system (*20*).

20-mers [5′ SH-$(CH_2)_6$-A_{10}-CAACTTCATC-CACGTTCAAC 3′], which are complementary with half of the target bar-code sequence, were used to capture the isolated bar-code DNA sequences, and oligonucleotide-modified 13-nm gold NPs = [5′ GCTAGTGAA-CACAGTTGTGT-A_{10}-$(CH_2)_3$-SH 3′-Au] were used to label the other half of the sequence in a sandwich assay format. Chips with hybridized NP probes are then subjected to silver amplification (*25*), which results in gray spots that can be read with a Verigene ID (identification) system (Nanosphere, Incorporated, Northbrook, IL) that measures light scattered from the developed spots. Target PSA concentrations from 300 fM to 3 aM

were detected with the use of the PCR-coupled approach (Fig. 2). The use of this approach in a more complicated medium such as goat serum provided a detection sensitivity of 30 aM, with clear differentiation from background signal (fig. S4). The selectivity for the bar-code DNA sequence was excellent, as evidenced by the lack of signal from the control spots with noncomplementary capture DNA [5′SH-$(CH_2)_6$-A_{10}-GGCAGCTCGTGGTGA 3′] and the observation that there is little discernible signal when PSA is absent (Fig. 2).

Importantly, one can eliminate the PCR step and still obtain a high sensitivity assay by using larger nanoparticles (30 nm), which can support larger absolute amounts of bar-code DNA. With such an assay, it was possible to detect PSA at 30 aM concentration in a 10-μl sample (Fig. 2, inset). This substantially simplifies the overall complexity of the assay and still yields a sensitivity that is five orders of magnitude greater than the cited commercial assay sensitivity (*19*) and two orders of magnitude greater than that cited for immuno-PCR on the same target under near-identical conditions (*13*).

The bio–bar-code method offers several advantages over current protein detection methods. First, the target-binding portion of the assay is homogeneous (in the sense that the capture antibodies on the MMPs are dispersed in solution as opposed to the flat surface of a microarray or titer plate). Therefore, we can add a large quantity of MMPs to the reaction vessel to facilitate the binding kinetics between the detection antibody and target analyte. Homogeneous mixing makes this assay faster than heterogeneous immuno-PCR systems and also can increase sensitivity because the capturing step is more efficient (the equilibrium can be pushed toward the captured protein state by increasing the concentration of MMP probe, which cannot be done in the heterogeneous assay). Second, the use of the NP bio–bar codes provides a high ratio of PCR-amplifiable DNA to labeling Ab that can substantially increase assay sensitivity. Third, this assay obviates the need for complicated conjugation chemistry for attaching DNA to the labeling Abs. Bar-code DNA is bound to the NP probe through hybridization at the start of the labeling reaction and liberated for subsequent identification with a simple wash step. Because the labeling Ab and DNA are present on the same particle, there is no need for the addition of further antibodies or DNA-protein conjugates before the identification of bar-code DNA. In addition, the bar-code DNA is removed from the detection assay, and direct detection or PCR is carried out on samples of bar-code DNA that are free from PSA, most of the biological sample, microparticles, and nanoparticles. This step substantially reduces background signal. Finally, this protein detection scheme has the potential for massive multiplexing and the simultaneous detection of many analytes in one solution, especially in the PCR-less form. Although the PSA system is used for the proof of concept, the approach should be general for almost any target with known Abs, and, by using the NP-based bio–bar-code approach (*7*), one could prepare a distinct identifiable bar code for nearly every target of interest.

References and Notes

1. R. K. Saiki *et al*., *Science* **230**, 1350 (1985).
2. R. A. Gibbs, *Curr. Opin. Biotechnol.* **2**, 69 (1991).
3. S. A. Bustin, *J. Mol. Endocrinol.* **29**, 23 (2002).
4. G. MacBeath, S. L. Schreiber, *Science* **289**, 1760 (2000).
5. H. Zhu *et al*., *Science* **293**, 2101 (2001); published online 26 July 2001; 10.1126/science.1062191.
6. B. B. Haab, M. J. Dunham, P. O. Brown, *Genome Biol.* **2**(2): research0004.1 (2001).
7. J.-M. Nam, S.-J. Park, C. A. Mirkin, *J. Am. Chem. Soc.* **124**, 3820 (2002).
8. T. Sano, C. L. Smith, C. R. Cantor, *Science* **258**, 120 (1992).
9. A. McKie, D. Samuel, B. Cohen, N. A. Saunders, *J. Immunol. Methods* **270**, 135 (2002).
10. H. Zhou, R. J. Fisher, T. S. Papas, *Nucl. Acids Res.* **21**, 6038 (1993).
11. E. R. Hendrickson, T. M. Hatfield-Truby, R. D. Joerger, W. R. Majarian, R. C. Ebersole, *Nucl. Acids Res.* **23**, 522 (1995).
12. C. M. Niemeyer *et al*., *Nucl. Acids Res.* **27**, 4553 (1999).
13. B. Schweitzer *et al*., *Proc. Natl. Acad. Sci. U.S.A.* **97**, 10113 (2000).
14. C. M. Niemeyer, *Trends Biotechnol.* **20**, 395 (2002).
15. J. L. Stanford *et al*., *Prostate Cancer Trends 1973–1995* [National Institutes of Health (NIH) Pub. No. 99-4543, Surveillance, Epidemiology, and End Results (SEER) Program, National Cancer Institute, Bethesda, MD, 1999].
16. M. H. Black *et al*., *Clin. Cancer Res.* **6**, 467 (2000).
17. R. A. Ferguson, H. Yu, M. Kalyvas, S. Zammit, E. P. Diamandis, *Clin. Chem.* **42**, 675 (1996).
18. L. A. G. Ries *et al*., *SEER Cancer Statistics Review 1973–1999* (SEER Program, National Cancer Institute, Bethesda, MD, 2002).
19. H. Yu, E. P. Diamandis, A. F. Prestigiacomo, T. A. Stamey, *Clin. Chem.* **41**, 430 (1995).
20. Detailed materials and methods can be found on *Science* Online.
21. C. A. Mirkin, R. L. Letsinger, R. C. Mucic, J. J. Storhoff, *Nature* **382**, 607 (1996).
22. Y. C. Cao, R. Jin, C. A. Mirkin, *Science* **297**, 1536 (2002).
23. For 13-nm NPs, each NP can support up to 100 strands of DNA with the proteins present (*26*); this value represents the upper limit, and the exact number for these particles has not yet been determined.
24. T. A. Taton, C. A. Mirkin, R. L. Letsinger, *Science* **289**, 1757 (2000).
25. Silver enhancement kit was purchased from Ted Pella (Redding, CA), and silver enhancement time was 6 min.
26. L. M. Demers *et al*., *Anal. Chem.* **72**, 5535 (2000).

27. C.A.M. acknowledges the Air Force Office of Scientific Research, the Defense Advanced Research Projects Agency, and the NSF for support of this research. C.S.T. acknowledges the Howard Hughes Medical Institute for a Training fellowship. A. Schaeffer is acknowledged for helpful discussions, and V. Levenson assisted in PCR optimization.

Supporting Online Material

www.sciencemag.org/cgi/content/full/301/5641/1884/DC1
Materials and Methods
Figs. S1 to S5
References and Notes

3 July 2003; accepted 28 August 2003

Particle Formation by Ion Nucleation in the Upper Troposphere and Lower Stratosphere

S.-H. Lee,[1]* J. M. Reeves,[1] J. C. Wilson,[1] D. E. Hunton,[2] A. A. Viggiano,[2] T. M. Miller,[2] J. O. Ballenthin,[2] L. R. Lait[3]

Unexpectedly high concentrations of ultrafine particles were observed over a wide range of latitudes in the upper troposphere and lower stratosphere. Particle number concentrations and size distributions simulated by a numerical model of ion-induced nucleation, constrained by measured thermodynamic data and observed atmospheric key species, were consistent with the observations. These findings indicate that, at typical upper troposphere and lower stratosphere conditions, particles are formed by this nucleation process and grow to measurable sizes with sufficient sun exposure and low preexisting aerosol surface area. Ion-induced nucleation is thus a globally important source of aerosol particles, potentially affecting cloud formation and radiative transfer.

Atmospheric aerosols affect climate directly by altering the radiative balance of the Earth (*1*) and indirectly by acting as cloud condensation nuclei (CCN) (*2*), which in turn change the number and size of cloud droplets and the cloud albedo. Homogeneous nucleation (HN) (formation of solid or liquid particles directly from the gas phase) is an important source of new particles in the atmosphere (*3*, *4*), but the process is poorly understood and alone is unable to explain the observed particle formation. Homogeneous nucleation includes binary homogeneous nucleation (BHN) of sulfuric acid–water (H_2SO_4-H_2O) (*3*, *4*) and ternary homogeneous nucleation

[1]Department of Engineering, University of Denver, Denver, CO 80208, USA. [2]Air Force Research Laboratory, Space Vehicle Directorate, Hanscom Air Force Base, MA 01731, USA. [3]National Aeronautics and Space Administration, Goddard Space Flight Center, Greenbelt, MD 20771, USA.

*To whom correspondence should be addressed. E-mail: shanlee@du.edu